Improving Tissue Preparation for Matrix-Assisted Laser Desorption Ionization Mass Spectrometry Imaging. Part 1: Using Microspotting

Julien Franck,[†] Karim Arafah,[†] Alan Barnes,[‡] Maxence Wisztorski,[†] Michel Salzet,[†] and Isabelle Fournier*[,†]

Université de Lille1, CNRS, Team, Laboratoire de Neuroimmunologie des Annélides, MALDI Imaging, F-59655 Villeneuve d'Ascq Cedex, France, and Shimadzu Corporation, Wharfside, Trafford Wharf Road, Manchester, U.K.

Nowadays, matrix-assisted laser desorption ionization mass spectrometry imaging (MALDI MSI) is a powerful technique to obtain the distribution of endogenous and exogenous molecules within tissue sections. It can, thus, be used to study the evolution of molecules across different physiological stages in order to find out markers or get knowledge on signaling pathways. In order to provide valuable information, we must carefully control the sample preparation to avoid any delocalization of molecules of interest inside the tissue during this step. Currently, two strategies can be used to deposit chemicals, such as the MALDI matrix, onto the tissue both involving generation of microdroplets that will be dropped off onto the surface. First strategy involves microspraying of solutions. Here, we have been interested in the development of a microspotting strategy, where nanodroplets of solvent are ejected by a piezoelectric device to generate microspots at the tissue level. Such systems allow one to precisely control sample preparation by creating an array of spots. In terms of matrix crystallization, a microspotting MALDI matrix is hardly compatible with the results by classical (pipetting) methods. We have thus synthesized and studied new solid ionic matrixes in order to obtain high analytical performance using such a deposition system. These developments have enabled optimization of the preparation time because of the high stability of the printing that is generated in these conditions. We have also studied microspotting for performing on-tissue digestion in order to go for identification of proteins or to work from formalin fixed and paraffin embedded (FFPE) tissue samples. We have shown that microspotting is an interesting approach for on tissue digestion. Peptides, proteins, and lipids were studied under this specific preparation strategy to improve imaging performances for this class of molecules.

Since its introduction in 1997 by the group of R. M. Caprioli et al.,[1] tissue profiling and imaging by matrix-assisted laser desorption ionization (MALDI) mass spectrometry has allowed the analysis of hundreds of biomolecules while maintaining tissue integrity and molecular localization.[2−4] The detection and mapping of several classes of biomolecules like proteins,[5−9] peptides,[10−14] and lipids[15−22] were then possible. In MALDI mass spectrometry imaging (MALDI MSI), the matrix is uniformly deposited on a fresh frozen tissue section and a pulsed laser irradiates the surface leading to desorption and ionization of compounds contained in discrete locations (profiling) or on a whole tissue section by rastering the pulsed laser (imaging).

* Corresponding author. E-mail: isabelle.fournier@univ-lille1.fr.
[†] Université de Lille1, CNRS.
[‡] Shimadzu Corporation.

(1) Caprioli, R. M.; Farmer, T. B.; Gile, J. *Anal. Chem.* **1997**, *69*, 4751–4760.
(2) Chaurand, P.; Schwartz, S. A.; Caprioli, R. M. *Curr. Opin. Chem. Biol.* **2002**, *6*, 676–681.
(3) Chaurand, P.; Stoeckli, M.; Caprioli, R. M. *Anal. Chem.* **1999**, *71*, 5263–5270.
(4) Rubakhin, S. S.; Greenough, W. T.; Sweedler, J. V. *Anal. Chem.* **2003**, *75*, 5374–5380.
(5) Seeley, E. H.; Caprioli, R. M. *Proc. Natl. Acad. Sci. U.S.A.* 2008.
(6) Chaurand, P.; Rahman, M. A.; Hunt, T.; Mobley, J. A.; Gu, G.; Latham, J. C.; Caprioli, R. M.; Kasper, S. *Mol. Cell. Proteomics* **2008**, *7*, 411–423.
(7) Lemaire, R.; Menguellet, S. A.; Stauber, J.; Marchaudon, V.; Lucot, J. P.; Collinet, P.; Farine, M. O.; Vinatier, D.; Day, R.; Ducoroy, P.; Salzet, M.; Fournier, I. *J. Proteome Res.* **2007**, *6*, 4127–4134.
(8) Schwamborn, K.; Krieg, R. C.; Reska, M.; Jakse, G.; Knuechel, R.; Wellmann, A. *Int. J. Mol. Med.* **2007**, *20*, 155–159.
(9) Cornett, D. S.; Mobley, J. A.; Dias, E. C.; Andersson, M.; Arteaga, C. L.; Sanders, M. E.; Caprioli, R. M. *Mol. Cell. Proteomics* **2006**, *5*, 1975–1983.
(10) Fournier, I.; Day, R.; Salzet, M. *Neuroendocrinol. Lett.* **2003**, *24*, 9–14.
(11) Brand, G. D.; Krause, F. C.; Silva, L. P.; Leite, J. R.; Melo, J. A.; Prates, M. V.; Pesquero, J. B.; Santos, E. L.; Nakaie, C. R.; Costa-Neto, C. M.; Bloch, C., Jr. *Peptides* **2006**, *27*, 2137–2146.
(12) DeKeyser, S. S.; Kutz-Naber, K. K.; Schmidt, J. J.; Barrett-Wilt, G. A.; Li, L. *J. Proteome Res.* **2007**, *6*, 1782–1791.
(13) Stoeckli, M.; Staab, D.; Schweitzer, A.; Gardiner, J.; Seebach, D. *J. Am. Soc. Mass Spectrom.* **2007**, *18*, 1921–1924.
(14) Rubakhin, S. S.; Churchill, J. D.; Greenough, W. T.; Sweedler, J. V. *Anal. Chem.* **2006**, *78*, 7267–7272.
(15) Shimma, S.; Sugiura, Y.; Hayasaka, T.; Hoshikawa, Y.; Noda, T.; Setou, M. *J. Chromatogr., B: Anal. Technol. Biomed. Life Sci.* **2007**, *855*, 98–103.
(16) Jackson, S. N.; Wang, H. Y.; Woods, A. S. *J. Am. Soc. Mass Spectrom.* **2007**, *18*, 17–26.
(17) Jackson, S. N.; Wang, H. Y.; Woods, A. S. *Anal. Chem.* **2005**, *77*, 4523–4527.
(18) Jackson, S. N.; Wang, H. Y.; Woods, A. S.; Ugarov, M.; Egan, T.; Schultz, J. A. *J. Am. Soc. Mass Spectrom.* **2005**, *16*, 133–138.
(19) Jackson, S. N.; Wang, H. Y.; Woods, A. S. *J. Am. Soc. Mass Spectrom.* **2005**, *16*, 2052–2056.
(20) Jones, J. J.; Borgmann, S.; Wilkins, C. L.; O'Brien, R. M. *Anal. Chem.* **2006**, *78*, 3062–3071.
(21) Woods, A. S.; Jackson, S. N. *AAPS J.* **2006**, *8*, E391–395.
(22) Puolitaival, S. M.; Burnum, K. E.; Cornett, D. S.; Caprioli, R. M. *J. Am. Soc. Mass Spectrom.* **2008**, *19*, 882–886.

Many developments have been undertaken to improve MALDI MSI. Selection of the matrix and of the matrix deposition mode is a crucial step for MALDI imaging. In fact, most of the matrixes are specific to a mass range or family of compounds which can be exhibited more in tissue samples than in classical MALDI experiments due to the complex mixture of compounds in tissue. In addition, matrix choice is important from the viewpoint of solvent used and the crystal formation. Solvents used must allow good solubilization of the matrix and an efficient extraction of compounds in the tissue. Moreover, matrix layer quality greatly influences the resulting spectra reproducibility quality and will determine MALDI-MSI sensitivity, spectral resolution, and spatial resolution of molecular images. It is therefore, crucial to control uniformity of deposition using the smallest volume as possible to avoid analyte delocalization as well as crystal size and homogeneity of distribution across the spot for higher spatial resolution and spot-to-spot reproducibility. The easiest approach for depositing the matrix is manually with a micropipet. This allows a fast preparation of the tissue with a good extraction and cocrystallization of compounds. This preparation, however, suffers from poor reproducibility and delocalization of molecules within the tissues, and this approach is generally only used for profiling experiments. Another matrix application method is by spray coating, providing a homogeneous deposition of the matrix over the tissue section. This can be obtained manually with a pneumatic sprayer[23,24] or by a robotic device.[25−27] The homogeneous deposition of small droplets provides the formation of matrix crystals smaller than the laser beam diameter allowing the acquisition of images with a high spatial resolution. However, manual spray is generally not very reproducible. In this way, Electrospray deposition of matrix is much more reproducible and really provides highly homogeneous polycrystalline matrix layers with extremely small crystals and should provide the lowest delocalization and the highest spatial resolution. This type of matrix deposition, however, results in drastically reduced solvent (and matrix) volume that can be far too low to provide good extraction and incorporation of analytes into matrix crystals. Thus, this method provides almost perfect layers of matrix crystals but very poor quality MS spectra in terms of signal intensity and the number of detected ions, notably peptides and proteins. Compromised systems have been found between minimizing analyte delocalization and providing smallest matrix crystals with a homogeneous distribution while keeping enough solvent to preserve analytical performances. A new automatic system, the ImagePrep by Bruker Daltonics, was recently developed that creates matrix aerosol by vibrational vaporization under controlled condition. This system monitors the different steps of matrix deposition, extraction, and drying and allows control of the matrix layer thickness. Other techniques, like matrix sublimation,[28] were used to uniformly cover a tissue section for imaging. Such methods can only be used for analysis of molecules with low molecular weight (typically lipids) as these do not require embedding (cocrystallization) in the matrix crystal lattice for the desorption/ionization process to occur.

Alternative methods to spraying methods can be used for matrix deposition. One of the alternatives is to apply micro- or even nanovolumes of matrix solutions to create microspots at the tissue section level. In microspotting methods, the tissue will be covered with an array of matrix microspots. In this case, analyte delocalization cannot exceed the size of the spot. The main advantages of this method are the high reproducibility of matrix deposition and the high quality of spectra that can be recorded owing to solvent volume allowing for analyte extraction and incorporation in matrix crystals. In microspotting methods, the spot diameter is generally ~150 μm. Microspotting allows for creating an ordered array of spots but also deposition on specific locations. Various strategies have been developed to supply small amounts of matrixes. Microspotting can be obtained using acoustic deposition[29] and inkjet printing[30−32] or using a modified nano LC−MALDI spotter.[33] Here, we have used an automated piezoelectric chemical inkjet printer (CHIP-1000, Shimadzu) to generate picoliter droplets. With the use of this automated spotting device, small droplets of solution are ejected by piezoelectric heads directly onto the tissue section to generate a raster of spots of about 150−200 μm spot diameter. Interestingly, such a system allows various tissue treatments to be successively applied on the same spots such as on tissue digestion followed by matrix deposition. The different strategies developed by combining microspotting using CHIP-1000 and MALDI are presented in Figure S-1 in the Supporting Information. In these experiments, we describe complete strategies for MALDI MSI of lipids, peptides, and proteins imaging and identification using the CHIP-1000 systems. We present the methodological developments and improvements made in order to provide robust and reproducible high-quality imaging of analytes on such a system. Many developments were required to reach a real and usable tool, including the search and synthesis of new MALDI matrixes that were compatible with such a microdeposition system.

EXPERIMENTAL PROCEDURE

Materials. α-Cyano-4-hydroxycinnamic acid (HCCA), sinapinic acid (SA), 6-aza-2-thiothymine (ATT), tifluoracetic acid (TFA), ethanol (EtOH), acetonitrile (ACN), chloroform, aniline (ANI), and water CHROMASOLV PLUS for HPLC (H_2O) were purchased from Sigma-Aldrich (Saint Quentin Fallavier, France). Sequencing grade modified trypsin, porcine enzyme was from Promega (Charbonnières-les-Bains, France).

Tissue Preparation. Thin 10 μm tissue sections were obtained from frozen rat brain using a cryostat Leica CM1510S (Leica Microsystems, Nanterre, France) and applied onto ITO-coated

(23) Reyzer, M. L.; Hsieh, Y.; Ng, K.; Korfmacher, W. A.; Caprioli, R. M. *J. Mass Spectrom.* **2003**, *38*, 1081–1092.
(24) Schwartz, S. A.; Reyzer, M. L.; Caprioli, R. M. *J. Mass Spectrom.* **2003**, *38*, 699–708.
(25) Sugiura, Y.; Shimma, S.; Setou, M. *Anal. Chem.* **2006**, *78*, 8227–8235.
(26) Chen, Y.; Allegood, J.; Liu, Y.; Wang, E.; Cachon-Gonzalez, B.; Cox, T. M.; Merrill, A. H., Jr.; Sullards, M. C. *Anal. Chem.* **2008**, *80*, 2780–2788.
(27) Jardin-Mathe, O.; Bonnel, D.; Franck, J.; Wisztorski, M.; Macagno, E.; Fournier, I.; Salzet, M. *J. Proteomics* **2008**, *71*, 332–345.
(28) Hankin, J. A.; Barkley, R. M.; Murphy, R. C. *J. Am. Soc. Mass Spectrom.* **2007**, *18*, 1646–1652.
(29) Aerni, H. R.; Cornett, D. S.; Caprioli, R. M. *Anal. Chem.* **2006**, *78*, 827–834.
(30) Baluya, D. L.; Garrett, T. J.; Yost, R. A. *Anal. Chem.* **2007**, *79*, 6862–6867.
(31) Groseclose, M. R.; Andersson, M.; Hardesty, W. M.; Caprioli, R. M. *J. Mass Spectrom.* **2007**, *42*, 254–262.
(32) Patel, S. A.; Barnes, A.; Loftus, N.; Martin, R.; Sloan, P.; Thakker, N.; Goodacre, R. *Analyst* **2009**, *134*, 301–307.
(33) Lemaire, R.; Desmons, A.; Tabet, J. C.; Day, R.; Salzet, M.; Fournier, I. *J. Proteome Res.* **2007**, *6*, 1295–1305.
(34) Lemaire, R.; Wisztorski, M.; Desmons, A.; Tabet, J. C.; Day, R.; Salzet, M.; Fournier, I. *Anal. Chem.* **2006**, *78*, 7145–7153.

conductive glass slides (Bruker Daltonics, Bremen, Germany). It has been shown that MS spectra quality depends generally from the chemical washing step. Lemaire and co-workers introduced the use of chloroform[34] to mainly remove phospholipids which can interfere in the spectra and create poor crystallization when analyzing peptides or proteins. Caprioli et al. showed the use of alcohol to fix the tissue and remove salts and lipids.[35] Thus, for peptides/proteins analysis, tissue sections were submitted to a washing step using cold EtOH 95% during 15 s followed by a washing step using chloroform during 1 min in order to remove abundant lipids. For lipids analysis, no washing procedure was used.

On Tissue Digestion. Automatic trypsin deposition was performed using a high accurate position chemical inkjet printer CHIP-1000 (Shimadzu, Kyoto, Japan). A volume of 20 nL of solution containing 20 μg/mL of trypsin in 20 mM NH_4HCO_3 buffer was applied on each spot spaced by 250 μm center to center. Five droplets of 100 pL were deposited at each spot per cycle, and then 40 iterations were necessary to obtain the total volume. The tissue section was then incubated for 2 h in a humid atmosphere at 37 °C.

Mass Spectrometry Imaging of Proteins. A volume of 10 nL of solution containing 20 mg/mL of sinapinic acid (SA) in ACN/aqueous TFA 0.1% (6:4, v/v) were deposited using the CHIP-1000. The spots were spaced by 250 μm center to center, and five droplets of 100 pL were deposited at each spot per cycle, and then 20 iterations were necessary to obtain the final volume. A solid ionic matrix SA/aniline was prepared just prior to use according to a rapid conversion procedure. Briefly, 8.1 μL (1 equivalent) of ANI was added to a solution containing 20 mg/mL (1 equivalent) of SA in ACN/aqueous TFA 0.1% (6:4, v/v). The solution was then agitated for several minutes before use. For rapid conversion, the matrix solution must be used within 1 day of preparation. Alternatively, stable matrix powder can be synthesized by a long conversion method. In such a case, 1 equivalent of ANI is added to 1 equivalent of SA dissolved in methanol (MEOH, 2.5 mg/mL). The solution is then stirred for 1 h, and the solvent was evaporated in a rotary evaporator for 45 min. The matrix powder is then placed in a desiccator for 30 min to eliminate residual solvent and stored at −20 °C. Just prior to the experiment, the matrix solution is prepared by dissolving 20 mg/mL of SA/ANI in a solution of ACN/aqueous TFA 0.1% (6:4, v/v). This solid ionic matrix was deposited using the CHIP-1000 according to the same parameters as for SA. Molecular images were acquired using an UltraFlex II MALDI-time-of-flight (TOF)/TOF instrument (Bruker Daltonics, Bremen, Germany) equipped with a Smartbeam laser having a repetition rate up to 200 Hz and controlled by FlexControl 3.0 (Build 158) software (Bruker Daltonics, Bremen, Germany). Images were performed in the positive linear mode, and MALDI MS spectra were acquired in the 2500−35 000 m/z range. A total of 500 laser shots were averaged at each spot at a laser frequency of 100 Hz. The images were saved and reconstructed using FlexImaging 2.1 (Build 15) (Bruker Daltonics, Bremen, Germany).

Mass Spectrometry Imaging of Peptides. A solution containing 10 mg/mL of HCCA in ACN/aqueous TFA 0.1% (6:4, v/v) was used as the matrix for peptides analysis. The total volume of matrix was set to 20 nL and was deposited directly on tissue or on tryptic spots using the CHIP-1000. Solid ionic matrix HCCA/aniline (HCCA/ANI) was used as the matrix and was prepared following the procedure established previously[36] and similarly to SA/ANI. Briefly 14.4 μL of ANI (1.5 equivalent) was added to a solution containing 20 mg/mL of HCCA (1 equivalent) in ACN/aqueous TFA 0.1%. The matrix can also be synthesized using the complete conversion protocol as described for SA/ANI but using 1.5 base equivalent for 1 acid equivalent. The total volume of this solid ionic matrix was set to 10 nL and was deposited directly on tissue or on tryptic spots using the CHIP-1000. The images were performed in positive reflector mode, and MALDI MS spectra were acquired in the 600−5000 m/z range. A total of 500 laser shots were averaged at each spot at a laser frequency of 100 Hz. The images were saved and reconstructed using FlexImaging 2.1.

Mass Spectrometry Imaging of Lipids. A solution containing 15 mg/mL of ATT in EtOH/H_2O (1:1, v/v) was used as the matrix for lipids analysis. The total volume of this matrix was set to 20 nL and was deposited directly on the tissue using the CHIP-1000. The images were performed in positive and negative reflector modes, and MALDI-MS spectra were acquired in the 300−3000 m/z range. A total of 500 laser shots were averaged and acquired at each spot at a laser frequency of 100 Hz. The images were saved and reconstructed using FlexImaging 2.1.

MS/MS Identification of Digested Tissues. MS/MS experiments on digested tissue were performed using the UltraFlex II MALDI-TOF/TOF instrument equipped with a LIFT III cell. For MS/MS experiments, parameters were set as follows: laser repetition rate was 100 Hz, ion source voltages were, respectively, 8 and 7.3 kV on the MALDI sample plate and the first electrode; the LIFT cell was pulsed from ground for electrodes 1 and 2 to 19 kV and in the last step, electrode 3 was decreased to 3.2 kV; the reflector end voltage was set to 29.5 kV and midgrid to 13.85 kV. For each MS/MS spectrum 5000 total shots were averaged including 1000 for parent ions and 4000 for fragments. The laser fluence was increased over the experiments for generating lower m/z fragments.

Data Analysis. Protein identification in databanks were performed using Biotools 3.0 (Build 1.88) software (Bruker Daltonics, Bremen, Germany) connected to Mascot 2.2.0.3 search engine and interrogating the Swiss-Prot Protein Knowledgebase Release 56.1 of September 2, 2008 (397 539 sequence entries, comprising 143 289 088 amino acids abstracted from 172 934 references) with oxidation as the variable modification and no fixed modification. Taxonomy was specified to be *Rattus norvegicus*. Trypsin was selected as the enzyme, and two missed cleavages were selected. The mass tolerance was set at 0.5 and 1 Da, respectively, for the MS and MS/MS.

RESULTS

Mass Spectrometry Imaging of Proteins. Analysis of proteins by MALDI-TOF is generally performed using SA as a matrix. SA has also proven to be useful for MALDI-MSI of proteins. Thus, imaging of proteins directly from tissue using the CHIP-1000 was first performed using a solution of SA at 10 mg/mL. A total of 40

(35) Seeley, E. H.; Oppenheimer, S. R.; Mi, D.; Chaurand, P.; Caprioli, R. M. *J. Am. Soc. Mass Spectrom.* **2008**, *19*, 1069–1077.

(36) Lemaire, R.; Tabet, J. C.; Ducoroy, P.; Hendra, J. B.; Salzet, M.; Fournier, I. *Anal. Chem.* **2006**, *78*, 809–819.

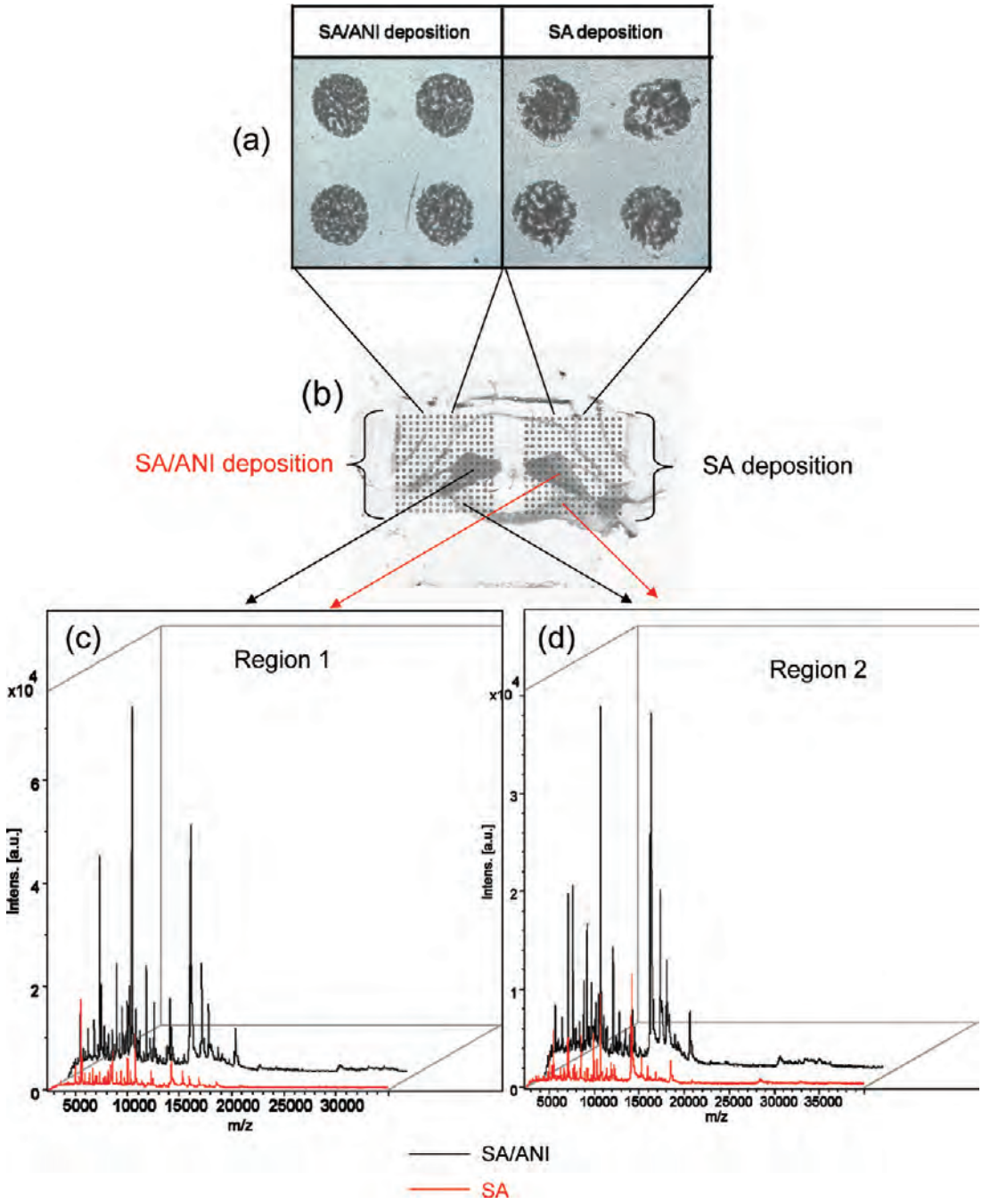

Figure 1. (a) Crystallization comparison between deposition of 10 nL of SA and deposition of 10 nL of SA/ANI, and (b−d) MS spectra recorded on two symmetric regions after deposition of 10 nL of SA/ANI and 10 nL of SA.

iterations were necessary to obtain a homogeneous crystallization on the tissue and a good signal in the MALDI-TOF spectrum. With dependence on the size of the tissue section, this number of iterations is time-consuming (approximately 2 h/cm^2). For this reason, the matrix concentration was increased up to 20 mg/mL, allowing for decreasing, thus, the number of iterations to 20 while keeping the same signal quality in the MALDI spectrum. The printing at this concentration was stable, and the spots were completely covered by a thin layer of SA. However, the MALDI-TOF/MS spectra were generally low in intensity and with a high background noise. Lemaire and coworkers[36] have shown that the use of solid ionic matrixes was providing a good alternative to "classical matrixes" for MALDI imaging. The use of solid ionic matrixes has been demonstrated to give better sensitivity, resolution, intensity, as well as better resistance to laser irradiation and lower matrix crystal sublimation under high vacuum conditions. Previously published work has shown solid ionic matrixes are better suited for peptide analysis from tissue sections.[36,37] In this work, a new solid ionic matrix SA/ANI was synthesized and tested as matrix to establish its efficiency to analyze proteins in tissues using the CHIP-1000 for matrix deposition and was compared to classical SA. Comparison of SA/ANI and SA was made from different levels including deposition, crystallization, and spectral aspects. Concerning matrix crystallization, the SA/ANI solid ionic matrix shows a more homogeneous crystallization than classical SA (Figure 1a). For SA, most of the spots present an external noncrystallized ring and a rather heterogeneous crystallization. For SA/ANI, spots are

Table 1. Intensity and Signal/Noise Values for Peptides and Proteins Detected by Microspotting

	intensity		S/N	
m/z	SA/ANI	SA	SA/ANI	SA
3 175.750	954.50	242.00	2.8	1.2
3 387.949	1 023.50	nd	3.0	nd
3 549.578	498.00	nd	1.4	nd
3 681.870	1 128.00	nd	3.3	nd
3 837.879	1 311.25	nd	3.8	nd
4 332.224	379.50	nd	1.1	nd
4 976.567	3 387.00	598.50	9.5	4.5
5 499.559	5 352.00	1 088.50	14.7	8.2
6 736.988	4 541.00	666.00	12.0	5.0
7 080.038	12 665.00	1 865.50	33.5	14.0
8 589.494	13 574.50	2 570.50	35.5	19.6
9 969.582	7 974.00	2 438.50	20.8	18.8
14 181.465	30 010.00	5 212.00	89.1	45.9
15 264.720	4 538.00	1 989.00	14.2	18.4
18 491.561	3 633.00	768.00	13.6	7.9
28 405.901	751.50	237.00	4.6	3.2

wholly covered by a thin homogeneous layer of matrix crystals. Moreover the spot diameter obtained from ionic matrixes is generally smaller. Because of the higher reproducibility and smaller spot diameter with SA/ANI, the distance between spots can be decreased. This enabled increasing the number of spots of the raster in the printed area and consequently to increase spatial resolution of images. In terms of the ease of deposition, both matrixes were similar in term of the stability of printing. Concerning MALDI MS, a comparison between SA and SA/ANI under microspotting conditions was performed on the same tissue section taking advantage of the brain symmetry to avoid artifact signal variations due to intersection composition variations or sample handling (Figure 1b). To carefully compare in detail the two matrixes, 5000 shots were accumulated in different regions of the tissue. As shown Figure 1c,d, spectral analysis clearly reveals that SA/ANI enables the detection of more signals over a broader *m/z* range. In particular, many peptides were observed in the low *m/z* range of the SA/ANI MS spectra when these signals were not observed for SA. Thus, SA/ANI provides spectra with a higher dynamic mass range. Ion signal intensities were also compared, and the intensities of several peaks over the *m/z* range are given in Table 1 for both matrixes. For the same laser energy just above the threshold for ion production, Table 1 shows that signal intensity and S/N is higher for the ionic matrix. This was confirmed for all the experiments. Up to a 5-fold increase in intensity was observed for certain peaks, and the signal intensity was always higher for SA/ANI. The averaged S/N ratio was 2-fold higher with SA/ANI. In conclusion, for equivalent printing stability, SA/ANI presents better crystallization and analytical performance than SA. SA/ANI spectra showed a higher number of peaks, of superior intensity, with a higher S/N ratio. SA/ANI was demonstrated to be more efficient for tissue analysis than SA and is a matrix to retain for MALDI MSI of proteins since it is also well suited with microspotting conditions. Figure 2 shows MALDI MSI experiments using SA/ANI after whole laser rastering of a rat brain tissue section under microspotting conditions.

(37) Djidja, M. C.; Francese, S.; Loadman, P. M.; Sutton, C. W.; Scriven, P.; Claude, E.; Snel, M. F.; Franck, J.; Salzet, M.; Clench, M. R. *Proteomics* **2009**, *9*, 2750–2763.

Over the whole tissue section (Figure 2a,b), very intense signals were observed with very specific spectrum profiles according to the acquisition position on the tissue. MALDI images of three different ions have been shown (Figure 2c). These compounds show the apparent different distribution in the rat brain section. Absolutely no delocalization of analytes was observed in the surrounding area outside of the tissue sample. MALDI matrixes better suited for proteins and peptides, in addition to performing well for imaging, accelerate the potential for biomarker discovery and tissue classification in disease samples.[38−40] In clinical applications, proteins that reveal a biologically relevant localization are of great interest. Consequently identification of proteins of interest is the next step after detection. The most direct strategy would be to fragment proteins to directly deduce their primary structure. Although, currently direct protein fragmentation is not possible for MALDI from complex mixtures because of compatibility with ion activation methods (low charge states) or parent ion selection (e.g., in-source decay (ISD)). Although, currently available methods allowing the generation of sufficient structural information from the direct fragmentation of proteins by various ion activation methods are either not available for MALDI (not enough charge states for ion transfer in some parts of the instrument) or with not enough efficiency (e.g., electron capture dissocaition (ECD)) because of the low charge states or efficiency but do not allow parent ion selection, requiring a purified sample (e.g., ISD on MALDI-TOF systems). Currently the most reliable method of protein identification from tissue samples is by enzymatic digestion followed by MS/MS of selected ions. Enzymatic digestion at the tissue level requires careful control of hydrolyzed peptide delocalization. Microspotting provides an excellent tool for controlling localization and volumes of enzymes in contact with the tissue sample. A "bottom-up" strategy involving an in situ enzymatic digestion has previously been shown using the chemical printer; however in these experiments, optimization of peptide detection conditions and trypsin digestion has been shown.

Mass Spectrometry Imaging of Peptides. Peptide analysis in MALDI MS is generally performed using either 2,5-dihydroxybenzoic acid (2,5-DHB) or HCCA as matrix. 2,5-DHB characteristically crystallizes in the shape of needles that grow from the outer rim of the deposited solution. In addition, a fine polycrystalline film forms in the inner part with salts species accumulating in this region. Because of this heterogeneous crystals distribution, 2,5-DHB is not best suited for MALDI MSI although this can be dependent on the method of deposition used. 2,5-DHB is compatible with spraying devices but has been shown to create heterogeneous crystallization when microspotted despite reduced crystal size and reduced heterogeneity than for classical MALDI sample preparation. 2,5-DHB is also known for presenting hot spots. This phenomenon can be overcome in classical MALDI by carefully and manually moving the sample under laser irradiation toward the needle part of the crystals. Because of the spatial resolution required in MALDI MSI, this is not possible to a large extent.

(38) Yao, I.; Sugiura, Y.; Matsumoto, M.; Setou, M. *Proteomics* **2008**, *8*, 3692–3701.

(39) Walch, A.; Rauser, S.; Deininger, S. O.; Hofler, H. *Histochem. Cell. Biol.* **2008**, *130*, 421–434.

(40) Deininger, S. O.; Ebert, M. P.; Futterer, A.; Gerhard, M.; Rocken, C. *J. Proteome Res.* **2008**, *7*, 5230–5236.

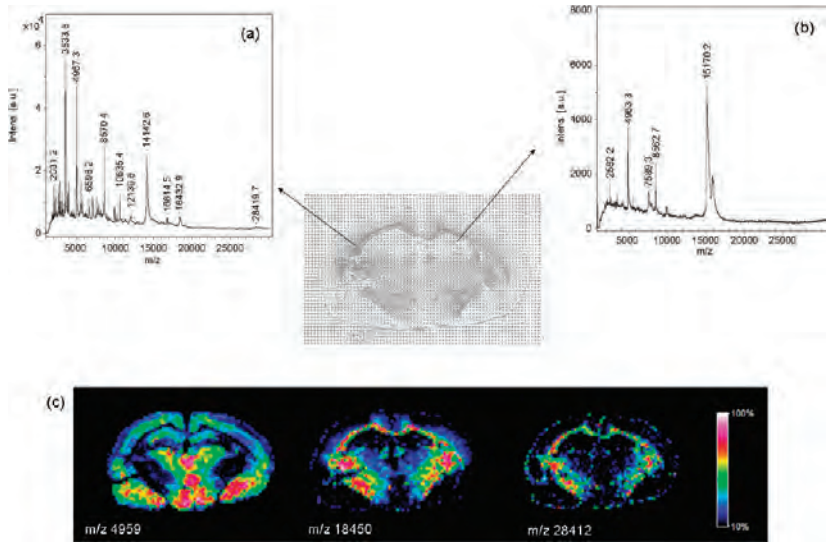

Figure 2. (a, b) MALDI MS spectra recorded in two different locations of a rat brain tissue section after automated microspotting of matrix solution (SA/ANI) and (c) reconstructed molecular images for *m/z* 4 959.3, *m/z* 18 450.7, and *m/z* 28 412.

For this reason, HCCA, which presents an homogeneous crystallization, was preferred to 2,5-DHB in these experiments. HCCA was used for microspoting by chemical printing. Pictures of rat brain tissue sections after the microspotting of HCCA are shown (Figure S-2a in the Supporting Information). The solution containing 10 mg/mL of HCCA was very difficult to spot. The printing was unstable after only 10 min of spotting leading to many satellite droplets, and the piezoelectric head was totally clogged after 30 min. To increase printing stability with HCCA, a cleaning procedure was required every 5 min. Alternatively the matrix solution concentration was decreased to 5 mg/mL, although for 5 mg/mL the number of iterations had to be increased therefore increasing the preparation time. Tissue microspotted with 5 mg/mL HCCA solution were analyzed but weak, and limited peptide signals were detected in addition to MS spectra showing high background noise. To overcome this drawback, solid ionic matrixes, HCCA/ANI or HCCA/DANI,[36] were tested under microspotting conditions. These matrixes have previously shown good sensitivity and a good intensity for peptide analysis from tissue sections. In addition, solid ionic matrixes benefit from high solubility and low surface tension, aiding the microspotting process. HCCA is difficult to solubilize at a concentration of 20 mg/mL in a mixture containing 60% ACN and 40% aqueous TFA 0.1%. An organic base, such as aniline, when added to the above solution, an acid−base reaction occurs and the complex is solubilized. We discovered that the higher solubility of the ionic matrix improved printing performance. In addition, we observed that crystallization time was longer with the ionic matrix, thus avoiding a rapid clogging of the piezoelectric head and possibly giving more time for better peptide extraction from tissues. A solution of HCCA/ANI containing 20 mg/mL of HCCA was then tested. Figure S-2b in the Supporting Information shows the pictures of a rat brain tissue section after HCCA/ANI microspotting. Comparison of HCAA and HCCA/ANI printing show that a well-defined raster of spots is obtained for HCCA/ANI, which was not possible for HCCA. It must also be noticed that for HCCA/ANI, the printing was stable over hours without requiring any cleaning procedure. Because of the benefits described above, solid ionic matrixes were chosen for imaging mass spectrometry of both endogenous peptides and peptides generated after enzymatic digestion. The classical proteomics approach to protein characterization involves extraction, fractionation of proteins, separation by RP-HPLC or by SDS PAGE, followed by an enzymatic digestion, and MS/MS analysis. Some groups have recently demonstrated the possibility to make protein identification after in situ enzymatic digestion followed by MS/MS directly on frozen[31] or FFPE tissues.[33,37,41,42] Identified proteins can then be cross-validated using classical immunohistochemistry or by a technique developed in our lab called TAG-MASS[43] allowing specific detection of proteins by MALDI-MSI (specific MALDI-MSI). Direct identification of proteins was performed by on-tissue microspotted enzymatic digestion. Advantages of chemical printer were great reproducibility for spotting different solutions at the same spot. In the case of enzymatic digestion, CHIP-1000 allowed, microdeposition of trypsin followed by incubation and a microspotting of HCCA/ANI matrix. Different concentrations of trypsin were tested from 20 μg/mL up to 100 μg/mL. No major differences in terms of the number of peptides detected after digestion were observed with varying trypsin concentration. The most apparent difference discovered was the presence of trypsin autolysis peaks which were most intense at 100 μg/mL trypsin concentration. However, even for the lowest concentration, autolysis peaks from trypsin at *m/z* 842.5, *m/z* 1045.5, *m/z* 2211.1, and *m/z* 2283.2 were still detected providing good internal calibration signals. The volume of solution required for printing was also taken into account. Generally, below 200 μL of solution loaded in the instrument led to droplets that were unstable and spotting became difficult. The amount of trypsin deposited was set to 40 nL per spot. Above this value, no difference was observed in terms of number of detected peptides even after 2 h incubation at 37 °C.

(41) Stauber, J.; Lemaire, R.; Franck, J.; Bonnel, D.; Croix, D.; Day, R.; Wisztorski, M.; Fournier, I.; Salzet, M. *J. Proteome Res.* **2008**, *7*, 969–978.
(42) Groseclose, M. R.; Massion, P. P.; Chaurand, P.; Caprioli, R. M. *Proteomics* **2008**, *8*, 3715–3724.
(43) Lemaire, R.; Stauber, J.; Wisztorski, M.; Van Camp, C.; Desmons, A.; Deschamps, M.; Proess, G.; Rudlof, I.; Woods, A. S.; Day, R.; Salzet, M.; Fournier, I. *J. Proteome Res.* **2007**, *6*, 2057–2067.

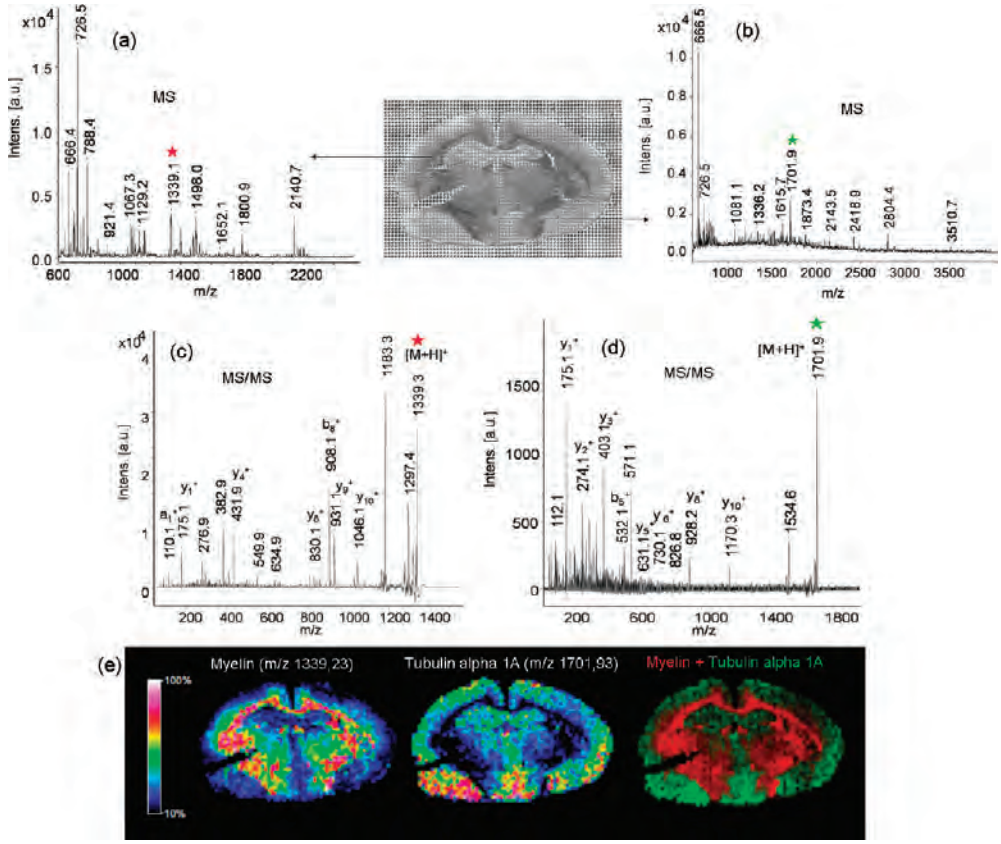

Figure 3. MALDI MSI of a rat brain tissue section after on-tissue trypsic digestion followed by matrix deposition (HCCA/ANI) using an automated microspotting device. (a, b) MS spectra recorded at two different locations of the tissue section and (c, d) corresponding MS/MS spectra of ions at *m/z* 1339.8 and *m/z* 1701.9. (e) Reconstructed molecular images for *m/z* 1339.8, *m/z* 1701.9, and overlaid image of both ions.

After in situ enzymatic digestion and image reconstruction, the peptides generated from the digest can be selected to perform MS/MS experiments for direct identification of proteins. Figure 3 shows the images of tryptic peptides indirectly giving the localization of the corresponding proteins indentified directly from the rat brain tissue section after enzymatic digestion and MS/MS experiments. In this example, two different proteins localized in different regions of the tissue were selected and directly submitted to MS/MS allowing one to correlate localization and identification of myelin and tubulin α 1A. These two proteins show a very specific localization and opposite distribution in the rat brain. Myelin is exclusively localized in the corpus callosum while tubulin α 1A is present in the rest of the tissue. This experiment also shows that microspotting of the enzyme followed by matrix deposition limited the delocalization of the species to the maximum value of the spot size. Taking into account the spot size as reference, the spatial resolution commonly obtain for microspotting is about 200 μm. Emphasis must also be given to the possibility to automatically move the laser over the spot during acquisition, which increases the sensitivity and S/N ratio. This is to be considered for MS/MS in order to improve fragmentation spectra quality for protein identification. This is also an opening to consider reconstructing digestion peptides images based on MS/MS spectra (specific fragments of peptides) and increasing image selectivity by avoiding isobaric ions overlapping effects that could be expected from the digestion of highly complex middles such as tissues. Taking advantage of the MS/MS discrimination power is the solution to image isobaric peptides belonging to different proteins presenting different distributions within the tissue.

Improving Deposition by Geometry Modification. In order to improve the printing reproducibility and quality of reagent deposition, we also studied the geometric parameters of the microspotter. We often observed that, due to the distance between the piezoelectric head and the sample, the deposition was sometimes not accurately reproducible possibly due to differences in solution viscosity. To overcome this drawback, we reduced and optimized the distance between the piezoelectric head and the sample by modifying the target holder used for printing. For this, an adapter for Prespotted AnchorChip targets from Bruker Daltonics was modified. A metal slide from approximately 1 mm of thickness is added directly on the target, and the slide containing the tissue section is then added on top of the metal slide using an adhesive tape as shown in Figure S-3 in the Supporting Information. By reduction of the distance, depositions were more accurate and reproducible allowing a better matrix deposition on the tryptic spots after an incubation step. This modification needed great care in order to avoid contact between the piezoelectric head and the slide. We also noticed that satellite spots (occasionally ejected by the piezoelectric heads) were observed less frequently due to the reduced distance for the satellite droplet to deviate from the principal spot. The accuracy of the deposit is thus greatly improved, and by combining this modification with the use of solid ionic matrixes such as SA/ANI

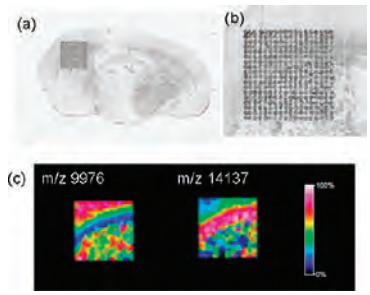

Figure 4. (a) Optical image of spots obtained after SA/ANI deposition using the CHIP-1000 with a spatial resolution of 150 μm. (b) Zoom of the region containing spots of SA/ANI. (c) Reconstructed molecular images for *m/z* 9 976 and *m/z* 14 137.

which present a highly stable printing, it is thus possible to decrease the spot size in order to improve the spatial resolution of images. By deposition of three droplets of SA/ANI by spot, a spatial resolution of 150 μm can be easily achieved (Figure 4a,b). A decrease in the spatial resolution is obtained without any alteration of the sensitivity (identical number of proteins detected with the same intensity). In Figure 4c is reported the reconstructed molecular images for two proteins, respectively, at m/z 9 976 and m/z14 137. These proteins have a close but not similar localization. This can be observed here using the highest resolution than with the classical microspotting conditions.

Improving Deposition Time. Microspotting has several advantages including multireagent deposition in specific locations and good control of analyte delocalization; however, the printing process is time-consuming. This is especially true when several reagents are successively spotted on a tissue section or for large samples. Previous MALDI imaging publications using microspotting devices have required an entire square or rectangular region to be printed (Figure S-4a, left panel in the Supporting Information). Printing areas that include regions outside the tissue can waste time and reagent. To remove these unnecessary regions, the simplest solution was to divide the printing area into several smaller areas of 4×4 spots. In this approach, spots were only on the tissue section and were following the shape of the tissue section (Figure S-4a, right panel in the Supporting Information). In all regions, reagents are spotted using the option "single pass iterative". With this option, a single pass is performed on the first small area before moving to the next. The benefit of performing printing by this method is that print positions have time for solvent to evaporate before the next printing round occurs, and through a number of iterations a sufficient quantity of solution is deposited. Optimization of printing time was also gained by increasing the frequency of the piezoelectric head from 240 (standard) to 960 Hz. This modification was only possible for extremely stable solutions such as solid ionic matrixes. Through the combined approach to printing optimization, over 1 h of printing time was saved for printing on a typical rat brain tissue section. Figure S-4b in the Supporting Information shows the images reconstructed after acquisition on rat brain tissue sections spotted with SA/ANI at high frequency and removing the unnecessary regions. The deposition was perfectly stable during the 20 passes with a high frequency, and the spots were well-defined and followed exactly the shape of the tissue section. The spectra quality and thus that of the resulting images (here, proteins) were not affected by these modifications.

Mass Spectrometry Imaging of Lipids. Since the emergence of the new field of lipidomics in early 2000,[44] "soft-ionization" mass spectrometer sources have became the optimal approach for lipid analysis of crude extracts. Direct profiling of lipids in tissue using a MALDI ion source was successfully reported[45] as well as MALDI MSI of a lipid distribution in brain tissue.[46,47] Despite the matrix clusters that occur in the low m/z ratio, a wide range of matrixes for lipidomic purpose have been compared for their crystallization, their acidic or neutral properties, and for their stability inside the MALDI source.[48] Because of its low background ions in the low mass range, stability under vacuum conditions, and quite large applicability to a broad range of lipid classes, the acidic organic matrix 2,5-DHB has become a well established matrix for lipid analysis in a biological mixture.[49] As previously described, 2,5-DHB is reputed for heterogeneity of crystallization and hot spots. Even when sprayed on a tissue, 2,5-DHB has been reported to be nonhomogeneous.[50] Despite this, depositing 2,5-DHB by a chemical printer achieved more homogeneous results than spraying. A. S. Woods et al. reported that the hydrophobic matrix 2,6-dihydroxyacetophenone (DHAP) and 6-aza 2-thithymine (ATT) matrix[17−19] gave better results for the direct analysis of lipids directly from tissue sections.[51]

Lipids are largely highly soluble in matrix solutions and can easily and quickly diffuse from tissues. Free solvent deposition of the matrix is a good alternative to minimize delocalization and generate a very thin and homogeneous crystallization polycrystalline layer,[22,28] although fewer lipid species are generally observed using such approaches. Microspotting however is again a good compromise between analytical performances and analyte delocalization. Microspotting was optimized for lipids imaging. Printing was successfully assessed for spotting ATT and DHAP matrix (Figure 5). The two matrixes ATT and DHAP were deposited onto a same rat brain slice. Half-left and half-right sides of the brain were, respectively, spotted with ATT and DHAP. An optical scanning of the slice was realized to observe matrix crystallization (Figure 5a) immediately after spotting of the matrixes. Tissues were also scanned after 1 h inside the MALDI source of the instrument under vacuum conditions (Figure 5b). As observed from these pictures, the microspots of DHAP matrix were sublimated under the MALDI source vacuum on the top and outside of the rat brain slice, whereas ATT matrix microspots were still present. So as to assess the behavior of these matrixes under high vacuum, spectra were recorded for each matrix in the rat brain just after microspotting and after 1 h under vacuum conditions. A comparison between lipids detected either with ATT or DHAP matrix was assessed in the rat brain (Figure 5c) in the positive reflector mode. Both matrix detected similar lipids in the studied m/z 700−900 and gave rise to high intensity signals of

(44) Han, X.; Gross, R. W. *J. Lipid Res.* **2003**, *44*, 1071–1079.
(45) Rujoi, M.; Estrada, R.; Yappert, M. C. *Anal. Chem.* **2004**, *76*, 1657–1663.
(46) Murphy, R. C.; Hankin, J. A.; Barkley, R. M. *J. Lipid Res.* 2008.
(47) Murphy, R. C.; Hankin, J. A.; Barkley, R. M. *J. Lipid Res.* **2009**, *50 Supplement*, S317–322.
(48) Schiller, B. F. a. J. *Eur. J. Lipid Sci. Technol.* **2009**, *111*, 83–98.
(49) Petkovic, M.; Schiller, J.; Muller, M.; Benard, S.; Reichl, S.; Arnold, K.; Arnhold, J. *Anal. Biochem.* **2001**, *289*, 202–216.
(50) Astigarraga, E.; Barreda-Gomez, G.; Lombardero, L.; Fresnedo, O.; Castano, F.; Giralt, M. T.; Ochoa, B.; Rodriguez-Puertas, R.; Fernandez, J. A. *Anal. Chem.* 2008.
(51) Wang, H. Y.; Jackson, S. N.; Woods, A. S. *J. Am. Soc. Mass Spectrom.* **2007**, *18*, 567–577.

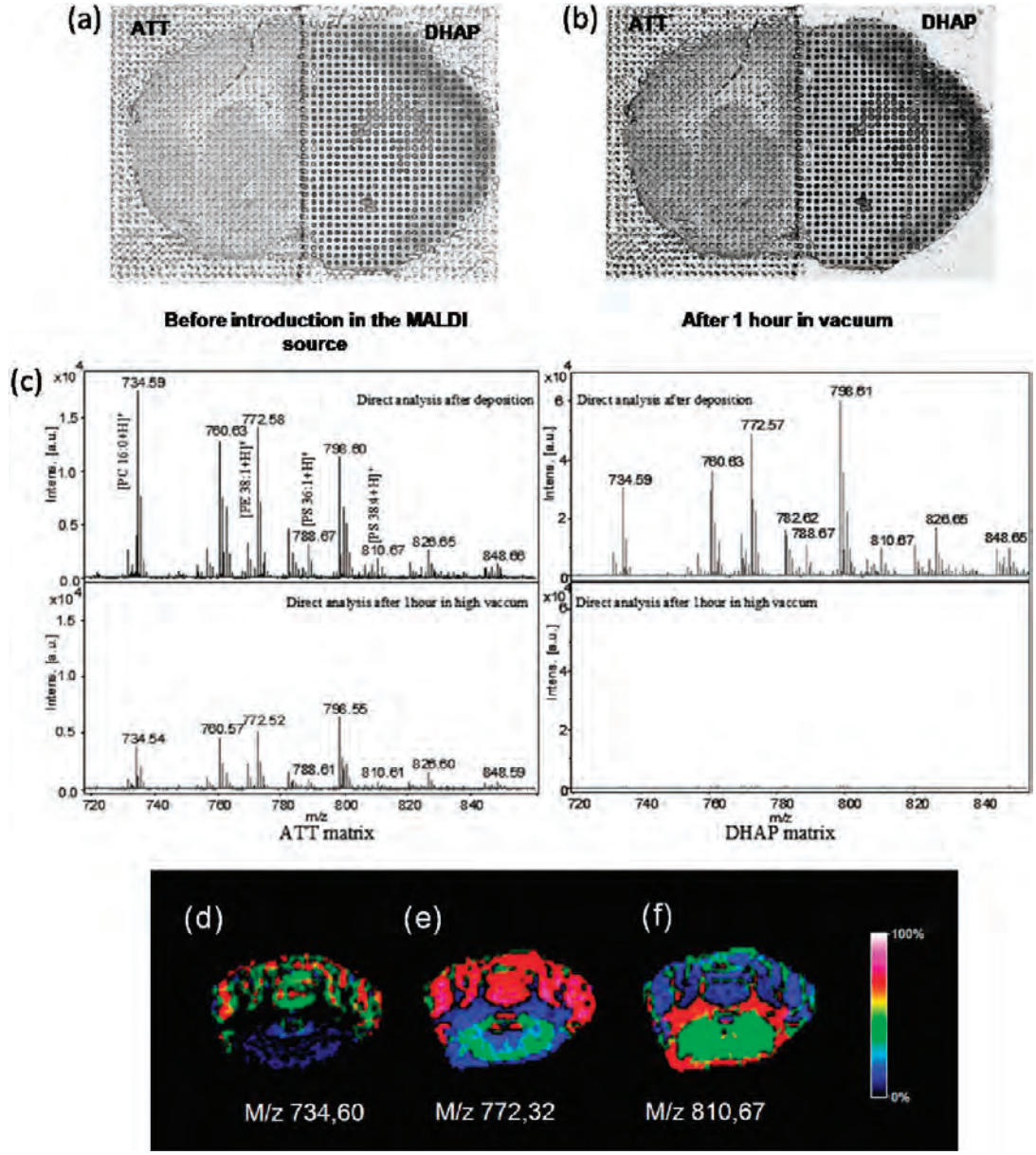

Figure 5. (a, b) ATT and DHAP matrix deposition onto a rat brain slice with the CHIP-1000 printer and vacuum-related effect on matrix sublimation. (c) Time-course vacuum effect on direct tissue analysis of lipids in white matter. Rat brain imaging of PC 16:0 (d), PE 38:1 (e), and PS 38:4 (f).

detected lipids when recorded immediately after introduction of the sample in the MALDI source. On the other hand, DHAP in high vacuum conditions for 1 h lead to a dramatic decrease in the intensity of the previous detected lipids whereas for ATT equivalent signal intensity is observed (Figure 5c). This highlights a previous observation made by A. S Woods et al.[52] regarding the sublimation of the DHAP matrix under high vacuum conditions. This sublimation is accentuated by the weak amount of DHAP matrix deposited onto the slice using the microspotting device. The stability of ATT matrix under high vacuum has taken advantage over DHAP for lipid imaging using a microspotting device.

With the knowledge that glycerophospholipids are extracted with a polar solvent such as ethanol, hand deposition of the matrix has been correlated with an important delocalization of this latter class of lipids.[21] As a consequence to these observations, the DHAP and ATT matrixes were used for microspotting. Because of its stability under vacuum conditions, only ATT was used for imaging sequences. The printer was set to generate 250 μm diameter spots of the ATT matrix. Spectra were then recorded in the positive reflector mode, and normalized images are presented (Figure 5d−f). MALDI images of $[M + H]^+$ ions of glycerophospholipids showed that phosphatidylcholine PC 16:0 (Figure 5d) and phosphatidylethanolamine PE 38:1 (Figure 5e) were observed mainly in gray matter, whereas phosphatidylglycerol PS 38:4 (Figure 5f) was located in white matter.

CONCLUSIONS

Sample preparation is a crucial step in the MALDI MSI workflow. The matrix choice and its crystallization is an important

(52) Jackson, S. N.; Woods, A. S. *J. Chromatogr., B: Anal. Technol. Biomed. Life Sci.* **2009**, *877*, 2822–2829.

parameter for MALDI MSI quality in terms of analytical performances but must be combined with an appropriate deposition method to avoid analyte delocalization. Minimization of analyte delocalization is tightly linked to the volume of solvent used. Minimization of solution volumes was the key to avoiding delocalization, but analytical performance (at least for peptides/proteins) was inversely related to larger volumes for ensuring their extraction and embedding in matrix crystals lattice. One of the deposition methods fulfilling both criteria was microspotting of solutions allowing the deposition of a small amount of solution at specific spots of defined diameter ensuring a delocalization at maximum of the size of the spot. Automatic microspotting allowed various reagents to be deposited on the tissue in a controlled manner. Identification strategies from tissue still currently require enzymatic digestion to generate peptides for MS/MS analysis. Moreover, N-terminal chemical derivatization of peptides can also be necessary for confident identification of proteins. Automatic microspotting ensured controlled experimental conditions which would be crucial when comparing sample replicates and extending to larger studies. We have shown in this article that reproducible, faster, and homogeneous deposition of reagents can be obtained for piezoelectric microspotting. After geometry modifications of the target, the printing realized higher reproducibility allowing a better deposition of different reagents at the same position. This was very useful in the case of in situ protein identification where trypsin was first deposited and then incubated before matrix deposition. Solid ionic matrixes for proteins and peptides, including new matrixes, were shown to be much more efficient and compatible with the printing. Solid ionic matrixes presented higher analytical performances in terms of sensitivity, number of detected compounds, signal intensity, S/N, stability under vacuum conditions but are also more suited with microspotting conditions with higher stability, reproducibility, and crystallization. Because of their lower crystallization speed and low vapor pressure, a better extraction of analytes from the tissue is hypothesized while no crystallization is observed on the piezoelectric head giving a stable printing during several hours. It was demonstrated that the deposition time could be improved by increasing the printing frequency with ionic matrixes and creating a region of interest following the shape of the tissue section. Enzymatic digestion was also optimized for printing conditions in order to provide efficient digestion while avoiding peptide delocalization. Better digestion yields are obtained by incubation after enzyme microspotting. Geometry optimization allowed one to more precisely add the matrix solution onto the enzyme spots. Combination of in situ enzymatic digestion with ionic matrixes allowed retrieving very rich peptide profiles with enough peak intensity for MS/MS experiments to be performed and to obtain high-quality spectra for protein identification.

By combination of the improvements concerning the printing, the chemical printer affords the possibility to detect lipids, peptides, and proteins in a high-throughput manner providing images with good spatial resolution and spectra of sufficient quality to perform statistical analysis.

ACKNOWLEDGMENT

This work was supported by grants from Centre National de la Recherche Scientifique (CNRS), Ministère de L'Education Nationale, de L'Enseignement Supérieur et de la Recherche, Agence Nationale de la Recherche (ANR PCV to I.F.), and Institut du Cancer (INCA to I.F.). Also supported by Conseil Régional Nord-Pas de Calais (grant to K.A.).

SUPPORTING INFORMATION AVAILABLE

Additional information as noted in text. This material is available free of charge via the Internet at http://pubs.acs.org.

Received for review June 29, 2009. Accepted August 10, 2009.

AC901328P